Editors' Suggestion | Featured in Physics

Bragg Diffraction of Large Organic Molecules

Christian Brand,[1,2] Filip Kiałka,[1,3] Stephan Troyer,[1] Christian Knobloch,[1] Ksenija Simonović,[1] Benjamin A. Stickler,[3,4] Klaus Hornberger,[3] and Markus Arndt[1,*]

[1]*University of Vienna, Faculty of Physics, Boltzmanngasse 5, A-1090 Vienna, Austria*
[2]*German Aerospace Center (DLR), Institute of Quantum Technologies, Söflinger Straße 100, 89077 Ulm, Germany*
[3]*Faculty of Physics, University of Duisburg-Essen, Lotharstraße 1, 47048 Duisburg, Germany*
[4]*QOLS, Blackett Laboratory, Imperial College London, SW7 2AZ London, United Kingdom*

(Received 14 June 2019; accepted 12 June 2020; published 16 July 2020)

We demonstrate Bragg diffraction of the antibiotic ciprofloxacin and the dye molecule phthalocyanine at a thick optical grating. The observed patterns show a single dominant diffraction order with the expected dependence on the incidence angle as well as oscillating population transfer between the undiffracted and diffracted beams. We achieve an equal-amplitude splitting of $14\hbar k$ (photon momenta) and maximum momentum transfer of $18\hbar k$. This paves the way for efficient, large-momentum beam splitters and mirrors for hot and complex molecules.

DOI: 10.1103/PhysRevLett.125.033604

Introduction.—Matter-wave diffraction and interference have numerous applications across the natural sciences. Electron and neutron diffraction are key techniques in condensed-matter physics and materials science [1,2], while atom interferometers are utilized in tests of fundamental physics, as well as for measuring physical constants and inertial forces [3,4]. Extending matter-wave interference experiments to large molecules enabled quantum-assisted studies of molecular properties [5,6] as well as the interference of biomolecules [7,8] and particles with masses beyond 25000 u [9].

One of the major techniques used in matter-wave interferometry is Bragg diffraction. It employs thick gratings [10] to coherently scatter the impinging particles into a single diffraction order. This allows for the realization of efficient matter-wave mirrors and beam splitters [11,12]. Bragg diffraction stands in contrast to Raman-Nath diffraction at thin gratings [13–15], which produces several diffraction orders arranged symmetrically around the incoming particle beam. Bragg diffraction was first demonstrated for neutrons [16] and later for atoms [17], Bose-Einstein condensates [18], electrons [19], and diatomic molecules [20].

Here, we report on the first Bragg diffraction of complex organic molecules. We show that the antibiotic ciprofloxacin and the dye molecule phthalocyanine [see Fig. 1(a)] can be reliably diffracted, despite being in a highly excited rotational state and possessing more than 100 vibrational degrees of freedom thermalized at 700–1000 K. This is an important step towards efficient coherent manipulation of functional, hot, and polar molecules.

Experimental setup.—The experimental setup is shown in Fig. 1(b): the molecules are evaporated by a focused laser beam, diffracted at a thick optical grating and collected on a quartz slide at the end of the vacuum chamber. In detail, a thin film of molecules is evaporated from the entrance window of a vacuum chamber by focusing a 420 nm laser beam down to a waist of 1.3(1) μm. We have used mass spectrometry to verify that molecular fragmentation can be neglected in the evaporation process [21]. After 1505 mm of free flight the molecular beam is transversely collimated with a piezocontrolled slit S_x, which we set to about 14 μm. After an additional 35 mm, the molecules are diffracted at a standing light wave, realized by retroreflecting a laser beam with wavelength $\lambda = 532$ nm, power $P \leq 14.6(2)$ W, and waist along the flight direction $w_z = 7.04(5)$ mm. The waist along y at the position of the molecular beam is set to $w_y = 55$–65 μm as measured with a fiber-based beam profiler [27]. The angle between the mirror surface and the molecular beam θ_{grat} is determined with an accuracy of about 5 μrad. This is achieved by finding the zero-incidence position of the actively stabilized piezo mirror mount and tilting it by the desired θ_{grat} before each run. Free fall in the gravitational field leads to a vertical dispersion of the molecular velocity at the detector surface. To ensure good velocity separation, a vertical slit S_y with an opening of 25 μm is placed about 20 mm in front of the grating. The slit is aligned with respect to the grating with an accuracy of 10 μm using the fiber-based profiler. The molecular diffraction pattern is collected on a quartz plate, 570 mm behind the grating and imaged using fluorescence microscopy [21]. The experiment is conducted at a pressure below 10^{-7} mbar to avoid collisional decoherence.

Ciprofloxacin is a polar biomolecule with a mass of $m = 331$ u and a negligible absorption cross section of $\sigma_{\mathrm{abs}} \ll 10^{-18}$ cm^2 for $\lambda \geq 400$ nm [28]. It interacts with the light grating via its optical polarizability volume $\alpha'_{532} = 38.9$ Å^3, which we calculated for the ground state

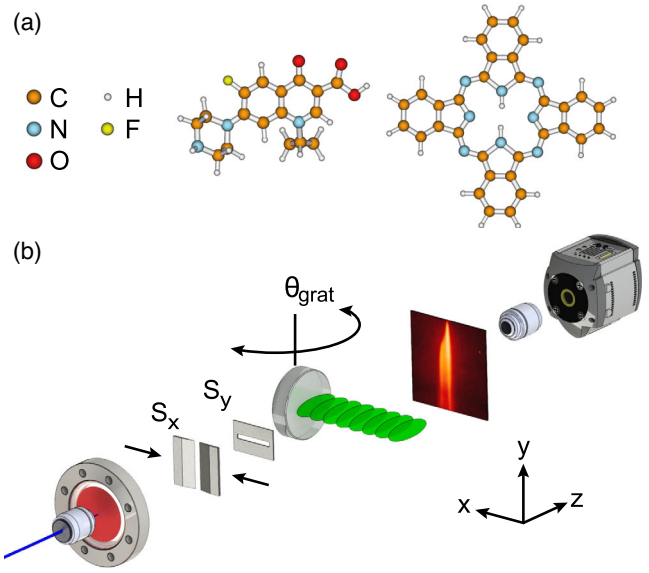

FIG. 1. (a) The experiments are performed with the antibiotic ciprofloxacin (left) and the organic dye phthalocyanine (right). (b) A thermal beam of molecules is produced by microevaporation and collimated vertically (S_x) and horizontally (S_y). After 1.5 m of free flight the molecules are diffracted at a thick laser grating created by retroreflecting a 532 nm laser at a highly reflective mirror. The angle of the mirror with respect to the molecular beam θ_{grat} can be controlled with μ rad precision. The molecular diffraction pattern is recorded after further 0.57 m of free flight by laser-induced fluorescence microscopy.

geometry at the PBE0/Def2TZVPP level. Phthalocyanine is a nonpolar dye molecule with a mass of $m = 515$ u and a static polarizability volume $\alpha' = 101$ Å^3 [29]. In contrast to ciprofloxacin, it has a non-negligible absorption cross section of $\sigma_{\mathrm{abs}} = 9 \times 10^{-18}$ cm^2 at 532 nm [30]. This allows us to observe the effect of absorption of the grating photons on the diffraction process.

Theoretical model.—Atomic and molecular Bragg diffraction follows from the induced dipole interaction of a polarizable point particle with a thick light grating. The particle moves initially with a velocity $\boldsymbol{v} = (v_x, v_y, v_z)$, where $v_z \gg v_x, v_y$. Since the forward momentum mv_z and the kinetic energy $m\boldsymbol{v}^2/2$ are much bigger than, respectively, the photon momentum $\hbar k = 2\pi\hbar/\lambda$ and the potential depth, the motion in the z direction is virtually unchanged by the grating and can be treated classically. The same can be assumed about the y motion. Furthermore, the high v_z allows us to neglect the free fall during the particle's passage through the grating. All this reduces the problem to the 1D dynamics along the x axis.

In a frame moving with the velocity v_x the particle is initially at rest while the grating is moving. The Hamiltonian can then be written as

$$\hat{H} = -\frac{\hbar^2}{2m}\frac{\partial^2}{\partial x^2} - V(t)\cos^2[k(x + v_x t)], \tag{1}$$

where $V(t) = 16P\alpha'/(cw_z w_y)\exp(-2v_z^2 t^2/w_z^2)$. The time-dependent Schrödinger equation $i\hbar\partial_t\psi(t,x) = \hat{H}\psi(t,x)$ can be solved using the ansatz

$$\phi(t,x) \equiv \exp\left(-\frac{i}{2\hbar}\int_{-\infty}^{t} dt' V(t')\right)\psi(t, x + \pi/2k) \tag{2}$$

$$= \sum_{j=-\infty}^{\infty} c_j(t) e^{ikjx/n}, \tag{3}$$

where $n \in \mathbb{N}$ is an arbitrary integer which determines the spacing between the basis states. For plane-wave illumination an $n = 1$ ansatz is sufficient; for numerical simulation with finite collimation, however, $n \gg 1$ is necessary. Substituting Eq. (3) into the Schrödinger equation yields the Raman-Nath equations [31],

$$ic_j' = \left(\frac{j}{n}\right)^2 c_j + \frac{\gamma}{4} e^{-2\tau^2/\sigma^2}\left[c_{j-2n} e^{4ip_{\mathrm{tr}}\tau} + c_{j+2n} e^{-4ip_{\mathrm{tr}}\tau}\right], \tag{4}$$

where a prime denotes a derivative over $\tau = \omega_r t$, $\omega_r = \hbar k^2/2m$, and

$$\gamma = \frac{V(0)}{\hbar\omega_r}, \qquad \sigma = \frac{w_z\omega_r}{v_z}, \qquad p_{\mathrm{tr}} = \frac{mv_x}{\hbar k}. \tag{5}$$

These correspond to dimensionless grating strength, interaction time, and momentum of the incident particle. The interaction time parameter is close to the ratio of the grating waist radius w_z and the characteristic length scale of near-field diffraction, the Talbot length $L_T = \lambda^2 mv/4h$ [32], for we have $\sigma = \pi w_z/4L_T$.

The Raman-Nath equations have approximate, closed-form solutions in the short-interaction and in the weak-potential limits. The thin-grating (or Raman-Nath) approximation amounts to dropping the kinetic term in Eq. (1), which is possible when the motion of the particle inside the grating can be neglected. This requires $\sigma p_{\mathrm{tr}} \ll 1$ and $\sigma\sqrt{\gamma} \ll 1$. In this regime the diffraction pattern is symmetric and independent of the incidence angle. The weak-grating (or Bragg) approximation amounts to the adiabatic elimination of all but two of the Raman-Nath equations. This is possible when the depth of the grating potential is small compared to the recoil energy, such that only transfer to the Bragg-reflected state is allowed by energy conservation. For $p_{\mathrm{tr}} > 1$ this is the case when $\gamma \ll 8(p_{\mathrm{tr}} - 1)$ [33]. In this regime, the interaction time necessary to achieve high-order diffraction grows like a factorial $\Gamma(p_{\mathrm{tr}})$, as the particle has to tunnel through increasingly many energy-forbidden states.

When the above approximations cannot be used, the solution can be obtained either via adiabatic expansion [33] or numerically. In our experiments with ciprofloxacin $\gamma \simeq 55$, $\sigma \simeq 0.38$, and $p_{\mathrm{tr}} \simeq 5$ (at 250 m/s), which lies in

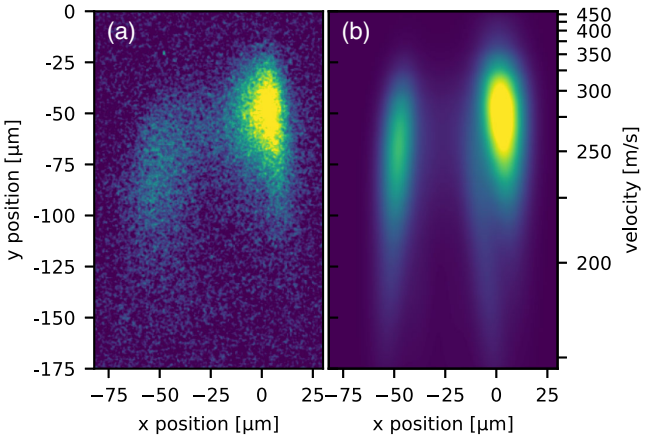

FIG. 2. False color image of the experimental (a) and simulated (b) Bragg diffraction pattern of the antibiotic ciprofloxacin. The laser grating waists are $w_z = 7.04(5)$ mm, $w_y = 55(5)$ μm, and the collimation slit is set to 14 μm.

this intermediate regime. We resort to numerical solution, since the convergence of the adiabatic expansion is slow. We note that in the intermediate regime both Raman-Nath-like and Bragg-like (also called quasi-Bragg [33]) diffraction can occur, depending on the intensity profile and the thickness of the grating [34]. We use a smooth Gaussian profile with sufficient thickness to demonstrate Bragg-like diffraction. The latter differs from diffraction in the weak-potential limit in that the intermediate diffraction orders are populated during the transit through the grating. This can lead to losses if the interaction time and strength are not optimally chosen. Finally, we note that classical dynamics of particles in sinusoidal potentials can give rise to analogous beam-splitting behavior [35]; however, a quantum model is generalizable and appropriate in the absence of plausible decoherence channels.

Diffraction of ciprofloxacin.—In Fig. 2(a) we show the pattern obtained by diffracting ciprofloxacin molecules at an incidence angle $\theta_{\mathrm{grat}} = -43(5)$ μrad. The y position in the image determines the forward velocity of the particles, which in turn determines the transverse momentum p_{tr} and the particle-grating interaction time σ.

For velocities above 300 m/s the interaction time is short compared to the inverse of the characteristic frequencies of the resonant Bragg transitions, and thus no diffraction occurs. As the characteristic frequencies increase sharply with decreasing p_{tr} [33], a relatively sudden onset of diffraction is observed at about 300 m/s. In the 300–150 m/s velocity range the molecules become consecutively resonant with the 6th–4th Bragg transition. The expected momentum transfer in a Bragg transition of order l is $2l\hbar k \propto v_z$. Since the flight time between the grating and the detector is inversely proportional to the forward velocity, we expect an approximately constant separation between the diffracted and the undiffracted beams. The slight bend in the diffracted beam results from the fact that the 6th order transition is dominant and thus contributes also at nonresonant velocities.

As the Bragg condition is relaxed by the limited interaction time, we observe no diffraction-free regions in between the resonances. Nevertheless, the appearance of a single diffracted beam and the asymmetry of the pattern help distinguish the observed phenomenon from stochastic photon absorption or Raman-Nath diffraction. We finally note that at $v_z \simeq 210$ m/s the amplitude of the diffracted beam matches that of the undiffracted one, demonstrating a $10\hbar k$ equal-amplitude beam splitter.

Numerical simulation using the Raman-Nath equations (4) [Fig. 2(b)] qualitatively reproduces the observed pattern [21]. The experimental and the simulated images are vertically aligned by matching the heights at which the diffracted peaks reach half of their maximal intensities. This determines the most probable velocity in the molecular beam of about 250 m/s.

Diffraction of phthalocyanine.—To explore the universality of molecular Bragg diffraction and its robustness to absorption, we switch to the dye molecule phthalocyanine. We quantify the absorption by setting θ_{grat} to an angle for which we do not expect diffraction and observing the broadening of the molecular beam. From the width of the beam we infer that on average one photon is absorbed inside the grating [21]. Despite the absorption, we obtain diffraction images of phthalocyanine, which are qualitatively similar to those of ciprofloxacin [see Fig. 3(a)]. The images exhibit oscillating population transfer [see Fig. 3(b)] reminiscent of the Pendellösung oscillations predicted by the theory of weak-potential Bragg diffraction and demonstrated with neutrons [36] and atoms [37]. Similar oscillations can be seen in the power dependence of the diffraction patterns [21].

To investigate the dependence of Bragg diffraction on the incidence angle, we record a series of diffraction images in which we vary θ_{grat} (see Fig. 4). In agreement with the expectations, we find the molecules diffracted to either side of the incoming beam, depending on the sign of the incidence angle. Similarly as for ciprofloxacin, the diffracted molecules form a slanted stripe indicating a single dominant transition. This transition is broadened by the 12 μrad collimation of the molecular beam [21], which results in deviations from specular reflection seen in Figs. 3 and 4. The highest momentum transfer recorded was $18\hbar k$ with an efficiency of 10% [Fig. 4(c)], and equal-amplitude splitting was realized for a momentum separation of $14\hbar k$ [Fig. 4(a)].

Discussion and outlook.—We have demonstrated Bragg diffraction for the complex organic molecules phthalocyanine and ciprofloxacin. As our data is in qualitative agreement with a simple polarizable-point-particle model, we expect that this technique can be applied without modification to any molecule of comparable size and absorption cross section. That is irrespective of the details

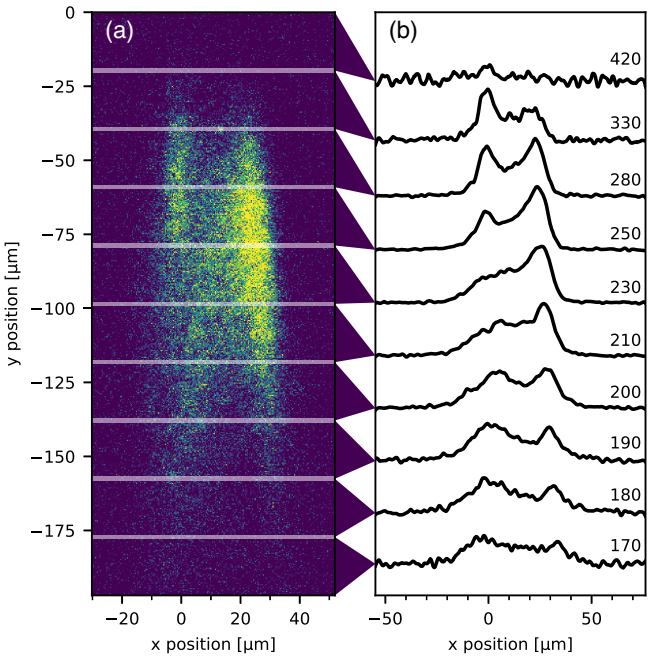

FIG. 3. Bragg diffraction pattern of the organic dye molecule phthalocyanine at an incidence angle $\theta_{\mathrm{grat}} = 5(5)$ μrad. Panel (a) shows the false color diffraction image. Panel (b) shows the averages of 20 μm high stripes, smoothed with median and Savitzky–Golay [38] filters, and annotated with their corresponding velocities in m/s. The velocities are determined by comparison with a diffraction pattern produced by a material grating [21]. The laser grating waist for this measurement is $w_y = 57(3)$ μm and the collimation slit width is 11.5 μm.

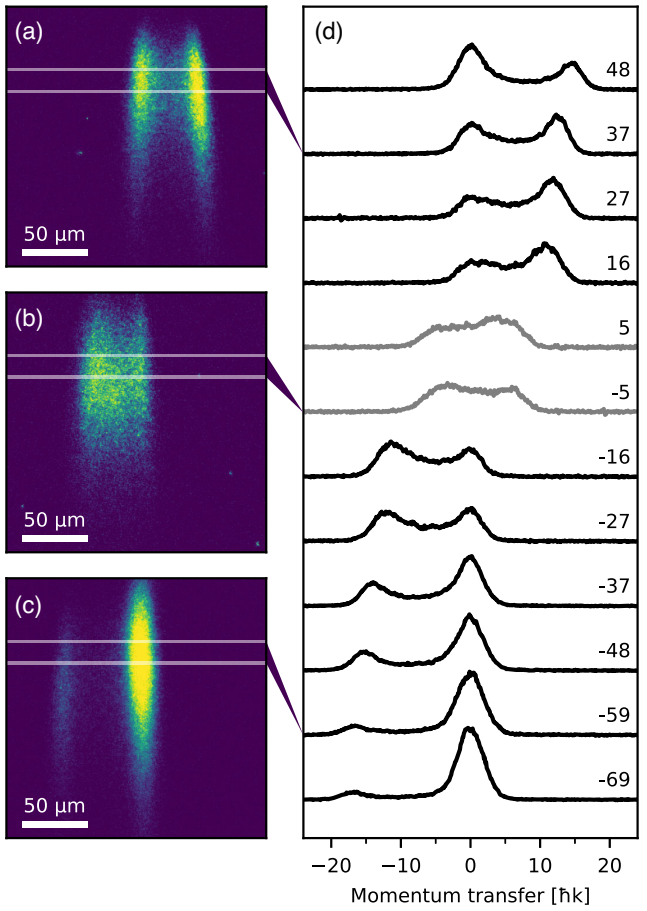

FIG. 4. Angular dependence of Bragg diffraction of the dye molecule phthalocyanine. Panels (a)–(c) show diffraction images for the incidence angles 48 (a), −5 (b) and −69 μrad (c). The images are 197 by 197 μm and the scale bars are 50 μm long. Panel (d) shows the integrated intensity profiles for the incidence angle varying from −69 to 48 μrad in steps of 10 μrad. The profiles are averages of 16 μm high stripes of the diffraction images corresponding to a velocity range of 234 to 255 m/s. The curves are horizontally aligned to center the undiffracted beam (which is the right peak for negative incidence and the left peak for positive incidence). For ±5 μrad we observe diffraction to both sides of the initial beam and hence align the traces with respect to their center of gravity. The laser grating waist for this measurement is $w_y = 65(5)$ μm and the collimation slit width is 14.8 μm.

of its electronic structure, dipole moment, etc. We have demonstrated a balanced beam splitter with a momentum separation of $14\hbar k$, which is to the best of our knowledge the largest equal-amplitude splitting demonstrated for molecules using optical gratings. Although with sufficient laser power similar or even greater splitting could be achieved with a thin optical grating, this would typically reduce the particle flux by a factor of 10 as only two of the many populated output beams have to be selected. The same problem applies to mechanical gratings, which additionally are incompatible with polar molecules due to rotational averaging.

Further development should increase the particle-grating interaction time in order to decrease losses and sharpen the Bragg resonances. A promising approach to achieve this is slowing the molecules using buffer gas cells [39]. This could ultimately allow for Mach-Zehnder interferometry with large molecules. The possibility to selectively address the arms in such a setup would, in turn, enable new interference schemes utilizing the molecules' chirality, conformation, and possibly entanglement between the molecules' internal and external degrees of freedom. Efficient Bragg diffraction could also enable pulsed Bloch oscillation beam splitters to realize even larger momentum transfers [40].

This project has received funding from the European Research Council (ERC) under the European Union's Horizon 2020 research and innovation program (Grant No. 320694) and the Austrian Science Fund (FWF) within Projects No. P-30176 and W1210-N25. We thank the Fetzer Pioneers' Fund (Project No. P#2018-1) for financial support, Armin Shayeghi for calculating the polarizability of ciprofloxacin, and Martin Fally for fruitful discussions. B. A. S. acknowledges funding from the European Union's Horizon 2020 research and innovation programme under the Marie Skłodowska-Curie Grant Agreement No. 841040.

*markus.arndt@univie.ac.at

[1] M. VanHove, W. Weinberg, and C. Chan, Low-Energy Electron Diffraction: Experiment, Theory and Surface Structure Determination, *Springer Series in Surface Sciences*, Vol. 6 (Springer-Verlag, Berlin, Heidelberg, 1986).

[2] Neutron Diffraction, *Topics in Current Physics*, edited by H. Dachs (Springer, Heidelberg, 1978).

[3] A. D. Cronin, J. Schmiedmayer, and D. E. Pritchard, Optics and interferometry with atoms and molecules, Rev. Mod. Phys. **81**, 1051 (2009).

[4] Atom Interferometry, in , *Proceedings of the International School of Physics "Enrico Fermi"*, edited by G. M. Tino and M. A. Kasevich (IOS Press, Amsterdam, Netherlands, 2014), Vol. 188.

[5] J. Tüxen, S. Gerlich, S. Eibenberger, M. Arndt, and M. Mayor, Quantum interference distinguishes between constitutional isomers, Chem. Commun. **46**, 4145 (2010).

[6] S. Eibenberger, X. Cheng, J. P. Cotter, and M. Arndt, Absolute Absorption Cross Sections from Photon Recoil in a Matter-Wave Interferometer, Phys. Rev. Lett. **112**, 250402 (2014).

[7] L. Mairhofer, S. Eibenberger, J. P. Cotter, M. Romirer, A. Shayeghi, and M. Arndt, Quantum-assisted metrology of neutral vitamins in the gas phase, Angew. Chem. Int. Ed. **56**, 10947 (2017).

[8] A. Shayeghi, P. Rieser, G. Richter, U. Sezer, J. H. Rodewald, P. Geyer, T. J. Martinez, and M. Arndt, Matter-wave interference of a native polypeptide, Nat. Commun. **11**, 1447 (2020).

[9] Y. Y. Fein, P. Geyer, P. Zwick, F. Kiałka, S. Pedalino, M. Mayor, S. Gerlich, and M. Arndt, Quantum superposition of molecules beyond 25 kDa, Nat. Phys. **15**, 1242 (2019).

[10] T. K. Gaylord and M. G. Moharam, Thin and thick gratings: terminology clarification, Appl. Opt. **20**, 3271 (1981).

[11] H. Müller, S.-w. Chiow, Q. Long, S. Herrmann, and S. Chu, Atom Interferometry with up to 24-Photon-Momentum-Transfer Beam Splitters, Phys. Rev. Lett. **100**, 180405 (2008).

[12] S.-w. Chiow, T. Kovachy, H.-C. Chien, and M. A. Kasevich, $102\hbar k$ Large Area Atom Interferometers, Phys. Rev. Lett. **107**, 130403 (2011).

[13] P. L. Gould, G. A. Ruff, and D. E. Pritchard, Diffraction of atoms by light: The near-resonant Kapitza-Dirac effect, Phys. Rev. Lett. **56**, 827 (1986).

[14] O. Nairz, B. Brezger, M. Arndt, and A. Zeilinger, Diffraction of Complex Molecules by Structures Made of Light, Phys. Rev. Lett. **87**, 160401 (2001).

[15] D. L. Freimund, K. Aflatooni, and H. Batelaan, Observation of the Kapitza-Dirac effect, Nature **413**, 142 (2001).

[16] D. P. Mitchell and P. N. Powers, Bragg reflection of slow neutrons, Phys. Rev. **50**, 486 (1936).

[17] P. J. Martin, B. G. Oldaker, A. H. Miklich, and D. E. Pritchard, Bragg scattering of atoms from a standing light wave, Phys. Rev. Lett. **60**, 515 (1988).

[18] M. Kozuma, L. Deng, E. W. Hagley, J. Wen, R. Lutwak, K. Helmerson, S. L. Rolston, and W. D. Phillips, Coherent Splitting of Bose-Einstein Condensed Atoms with Optically Induced Bragg Diffraction, Phys. Rev. Lett. **82**, 871 (1999).

[19] D. L. Freimund and H. Batelaan, Bragg Scattering of Free Electrons Using the Kapitza-Dirac Effect, Phys. Rev. Lett. **89**, 283602 (2002).

[20] J. R. Abo-Shaeer, D. E. Miller, J. K. Chin, K. Xu, T. Mukaiyama, and W. Ketterle, Coherent Molecular Optics Using Ultracold Sodium Dimers, Phys. Rev. Lett. **94**, 040405 (2005).

[21] See Supplemental Material at http://link.aps.org/supplemental/10.1103/PhysRevLett.125.033604 for details and Refs. [22–26] included therein.

[22] C. Knobloch, Coherent matter-wave manipulation techniques, Ph.D. thesis, University of Vienna, Austria, 2019.

[23] T. Juffmann, A. Milic, M. Müllneritsch, P. Asenbaum, A. Tsukernik, J. Tüxen, M. Mayor, O. Cheshnovsky, and M. Arndt, Real-time single-molecule imaging of quantum interference, Nat. Nanotechnol. **7**, 297 (2012).

[24] J. P. Cotter, C. Brand, C. Knobloch, Y. Lilach, O. Cheshnovsky, and M. Arndt, In search of multipath interference using large molecules, Sci. Adv. **3**, e1602478 (2017).

[25] J. Johansson, P. Nation, and F. Nori, QuTiP: An open-source Python framework for the dynamics of open quantum systems, Comput. Phys. Commun. **183**, 1760 (2012).

[26] J. Johansson, P. Nation, and F. Nori, QuTiP 2: A Python framework for the dynamics of open quantum systems, Comput. Phys. Commun. **184**, 1234 (2013).

[27] C. Brand, K. Simonović, F. Kiałka, S. Troyer, P. Geyer, and M. Arndt, A fiber-based beam profiler for high-power laser beams in confined spaces and ultra-high vacuum, Opt. Express **28**, 6164 (2020).

[28] C.-C. Lin and M.-S. Wu, Degradation of ciprofloxacin by UV/S2O82− process in a large photoreactor, J. Photochem. Photobiol. A **285**, 1 (2014).

[29] R. Ramprasad and N. Shi, Polarizability of phthalocyanine based molecular systems: A first-principles electronic structure study, Appl. Phys. Lett. **88**, 222903 (2006).

[30] H. Du, R.-C. A. Fuh, J. Li, L. A. Corkan, and J. S. Lindsey, PhotochemCAD: A computer-aided design and research tool in photochemistry, Photochem. Photobiol. **68**, 141 (1998).

[31] C. V. Raman and N. S. Nagendra Nath, The diffraction of light by high frequency sound waves: Part IV, Proc. Indian Acad. Sci. **3**, 119 (1936).

[32] H. F. Talbot, Facts relating to optical science. No. IV, Lond. Edinb. Dubl. Philos. Mag. **9**, 401 (1836).

[33] H. Müller, S.-w. Chiow, and S. Chu, Atom-wave diffraction between the Raman-Nath and the Bragg regime: Effective Rabi frequency, losses, and phase shifts, Phys. Rev. A **77**, 023609 (2008).

[34] C. Keller, J. Schmiedmayer, A. Zeilinger, T. Nonn, S. Dürr, and G. Rempe, Adiabatic following in standing-wave diffraction of atoms, Appl. Phys. B **69**, 303 (1999).

[35] P. Ryytty and M. Kaivola, Pulsed Standing-Wave Mirror for Neutral Atoms and Molecules, Phys. Rev. Lett. **84**, 5074 (2000).

[36] C. G. Shull, Observation of Pendellösung Fringe Structure in Neutron Diffraction, Phys. Rev. Lett. **21**, 1585 (1968).

[37] M. K. Oberthaler, R. Abfalterer, S. Bernet, C. Keller, J. Schmiedmayer, and A. Zeilinger, Dynamical diffraction of atomic matter waves by crystals of light, Phys. Rev. A **60** 456, (1999).

[38] A. Savitzky and M. J. E. Golay, Smoothing and differentiation of data by simplified least squares procedures, Anal. Chem. **36**, 1627 (1964).

[39] J. Piskorski, D. Patterson, S. Eibenberger, and J. M. Doyle, Cooling, Spectroscopy and Non-Sticking of trans-Stilbene and Nile Red, Chem. Phys. Chem. **15**, 3800 (2014).

[40] M. Ben Dahan, E. Peik, J. Reichel, Y. Castin, and C. Salomon, Bloch Oscillations of Atoms in an Optical Potential, Phys. Rev. Lett. **76**, 4508 (1996).